Contents lists available at ScienceDirect

Diamond & Related Materials

Reduction of amorphous carbon clusters from the highly disordered and reduced graphene oxide NPs by acoustical shock waves — Towards the formation of highly ordered graphene

A. Sivakumar [a], Lidong Dai [a,*], S. Sahaya Jude Dhas [b], S.A. Martin Britto Dhas [c], V. Mowlika [d], Raju Suresh Kumar [e], Abdulrahman I. Almansour [e]

[a] Key Laboratory of High-temperature and High-pressure Study of the Earth's Interior, Institute of Geochemistry, Chinese Academy of Sciences, Guiyang, Guizhou 550081, China
[b] Department of Physics, Kings Engineering College, Sriperumbudur, Chennai, Tamil Nadu 602 117, India
[c] Shock Wave Research Laboratory, Department of Physics, Abdul Kalam Research Center, Sacred Heart College, Tirupattur, Tamil Nadu 635 601, India
[d] Department of Physics, St Joseph's College of Arts and Science for Women, Hosur, Krishnagiri, Tamil Nadu 635 126, India
[e] Department of Chemistry, College of Science, King Saud University, P.O. Box 2455, Riyadh 11451, Saudi Arabia

ARTICLE INFO

ABSTRACT

The journey of exploring the acoustical shock wave-induced solid state phase transitions on polymorphic and allotropy materials have gained enormous momentum in recent years after the invention of the tabletop Reddy tube, but, the knowledge of shock wave-induced phase transitions on allotropy materials is very limited in comparison to the polymorphic materials. Hence, in this framework, we report the shock wave-induced transitions based on the reduction of the amorphous carbon clusters in the highly disordered and reduced graphene oxide nanoparticles (rGO NPs) [rGO — is also called as modified graphene]. The reduction of the disordered carbon in the rGO NPs under shocked conditions is examined by the techniques such as X-ray diffractometry and Raman spectrometer. X-ray crystallographic studies clearly present that as the shock pulses are increased, the intensity of the (002) peak is increased for which the authentication is observed by the Raman spectral analyses wherein it is clearly indicated the decrement and increment of the D and G bands against the exposure of the shock pulses thereby the I_D/I_G ratios are found to be 1.24, 1.17, 1 and 0.927 for 0, 100, 200 and 400 shocks, respectively. According to the Raman spectral results, the area of the amorphous Raman peak is reduced against the shock pulses such that the values are 98, 82, 81 and 48 for the 0, 100, 200 and 400 shocks, respectively. The removal of amorphous carbon clusters in the rGO NPs can be explained on the basis of the conversion of sp^3 to sp^2 hybridizations based on the shock wave induced hot-spot nucleation mechanism.

1. Introduction

Materials influenced by shock waves could contribute to the flamboyant, innovative and inspiring advancements in various fields because of the impact of shock waves which are capable of triggering phase transitions of various kinds such as structural, phase, morphological, magnetic, electrical, optical, molecular, etc. in functional materials [1–5]. In recent years, experimental methods that are available could allow materials for investigation whereby it is feasible to analyze at several bar pressure and temperature of a few thousands of Kelvin. Due to shock wave transient pressure, the formation of new phases, phase changes, material deformation, changes in electronic structure and

morphology can occur. Under extreme conditions, pressure and temperature are extremely high which could be tracked in high energy rays irradiation, high stress, high velocity electron irradiation and sudden dynamic impact conditions. In such extreme conditions, the probable crystallographic phases of all the familiar materials in the universe are not known [6–8]. Hence, the understanding of the structural stability of the known materials with respect to their crystallographic phase under extreme conditions is highly crucial such that this kind of research route can provide a platform by which the exploration on the features of Physics and Chemistry of the materials could be achieved thereby the possibility of finding new crystallographic structures might be ensured. Consequently, based on the above-mentioned claims, a lot of researchers

---

have been working worldwide over the last few decades and could find a lot of new materials of non-stoichiometry chemistry with very good functional properties [9–12]. In the series of silicon (Si), boron (B), germanium (Gi), antimony (Sb) and carbon elements based materials, there have been a large volume of studies carried out in the static pressure and temperature conditions [13–17]. But, after the discovery of the carbon nanotubes, the applications of the carbon-based materials have received a great deal of interest in both sides of technological aspects as well as academic aspects. Because, carbon is one of the best elements from the applications point of view such that it exhibits a wide spectra of different structures based on the bonding of carbon atoms [18–20] for which the stability profiles and defect engineering with respect to the structures are quite known at static high pressure [21,22] other extreme conditions such as laser irradiation, microwaves and high temperature [23–25] whereas the similar details are not sufficiently known under dynamic acoustic shocked conditions such that the most relevant results are reported here. Arman et al. have studied the molecular simulation studies of dynamic shock compression response of the carbon nanotube composites and found the deformation in carbon nanotubes at 4 GPa pressure [26]. Milyavskiy et al. have performed the structural stability of the C_{60} fullerite at shock compression for the range of 6–25 GPa pressure and found a series of phase transitions wherein the prominent transition from graphite-like carbon to a diamond-like phase has been observed at 25 GPa [27]. David Veysset et al. have examined the structural stability of the ordered graphite by the laser shock wave irradiation (A laser excitation pulse of 300 ps duration, 800 nm wavelength and laser excitation fluence of 24.0 J/cm^2) and found significant disordered graphite after the irradiation. As listed here, there have been several researchers who have examined carbon-based materials using various experimental approaches of the shock compression as well as laser shock waves and found mostly a similar kind of order-disorder type phase transitions [28]. Moreover, most of the static high pressure researchers have also observed a similar kind of ordered to the disordered phase transitions of graphene and graphite NPs [21,22] and there could be found a few articles related to the shock wave-induced phase transitions on graphite to diamond formation [29,30] and the conversion efficiency of the diamond phase and the lifetime of this phase is yet to be explored. Because, most of the experiments performed under shock compression experiments confirm the formation of the diamond from the graphite, while at the de-compressed state, the diamond phase disappears due to its elastic nature of phase transitions. But, in the case of the impact of shock wave research on materials [31–35], most of the researchers have found the plastic type phase transitions and due to its spectacular advantage, the dynamic acoustical shock wave loading process on materials has transformed into a very hot research topic in recent years such that several plastic type phase transition have been reported on a wide spectra of materials such as metal oxides [31], sulfates [32], ferrites [33], carbonates [34] and amino acids [35] and a very few reports have been made on the carbon materials. Using a conventional shock tube, traces of diamond nanoparticles have been noticed from the graphitic thin films by the influence of acoustical shock waves processing [36]. On the one hand, Biennier et al. have examined the shock wave processing of crystalline C_{60} in the hydrogen atmosphere and found the amorphous phase carbon at 2540 K shock temperature [37]. On the other hand, Arijit Roy et al. have demonstrated the transition from the amorphous to the crystalline carbon with several morphological patterns (For ex: nano ribbons, nanotubes) at a very high shock temperature 7300 K of hydrogen-free environment [38]. Very recently, our research group has performed the acoustical shock waves processing on the amorphous multi-wall carbon nanotubes using a tabletop Reddy Tube (transient temperature is 644 K and transient pressure is 1.0 MPa) and found the enforcement of crystalline nature in multi-wall carbon nanotubes [39]. Surfing through the overall literature reports on the shock wave processing with respect to the carbon-based materials, the occurrence of the ordered to the disordered type phase transitions is quite known which is quite common in all extreme conditions. Whereas, the disordered to the ordered phase transition is quite uncommon and the understating of this type of the phase transitions for the carbon materials remains to be an area that has to be ventured into thereby a lot of new potential information could be a possibility. Based on the above-mentioned claims, in the present work, we examine the shock wave processing on the amorphous reduced graphene oxide NPs to acquire more understanding about the disordered to the ordered phase transition enforced by the acoustical shock waves. To date, no report has been found on the shock wave processing for the crystalline as well as the amorphous phase reduced graphene oxide NPs.

In this work, we report the conversion of the amorphous phase to the crystalline phase of rGO by applying low shock pressure/temperature using the acoustical shock waves such that the results and discussions are drawn by X-ray and Raman spectroscopic analyzes.

2. Experimental procedures

GO has been typically synthesized from graphite by the modified Hummers and Offeman method. rGO is produced by the reduction of GO with sodium borohydride $NaBH_4$ following the standard procedure [40]. After obtaining the powder rGO samples, it has been subdivided into four equal parts such that one part has been kept as the control sample while the rest of the samples have been made use of for the shock wave impact analyses. For the experimental analysis, Mach number 2.2 shock waves (transient pressure and temperature of 2.0 M Pa and 864 K) have been preferred such that three different set of shock pulses with the counts of 100, 200 and 400 shocks have been exposed on those three samples, respectively. The shock waves have been generated utilizing a semiautomatic Reddy tube. The reported findings [32–34] account for the expanded version of the methodology for the working of a shock tube and the shock wave loading procedure. After the completion of the shock wave impact procedures, the shock wave loaded samples and the control sample have been fixed for the respective characterizations of powder X-ray diffraction, Raman spectroscopic and vibrating sample magnetometric analyses to be carried out.

3. Results and discussion

3.1. X-ray diffraction analysis

Powder X-ray diffractometer has been utilized to examine the rGO samples' degree of crystalline nature such that the recorded XRD patterns of the control and acoustical shock wave treated samples are shown in Fig. 1a. Based on the obtained control rGO sample's XRD pattern, a broad peak is identified at 26.6° which clearly represents the formation of the amorphous phase reduced graphene oxide such that there is no detectable crystalline phase in the XRD pattern wherein the formation of the amorphous phase is fully occupied by the sp^3 carbon atoms [28,39]. The observed XRD pattern of the control rGO sample is found to be well-matched with the previously reported amorphous phase rGO NPs. As seen in Fig. 1, at 100 shocked conditions, the tiny crystalline peak's (002) intensity is slightly increased when compared to the control rGO sample which means that the degree of crystalline nature of the existed amorphous phase rGO is slightly increased by the influence of the shock waves. Surprisingly, while increasing the number of shock pulses to 200, and 400, a considerable growth is witnessed in its peak intensity at every stage of increasing shock number and the corresponding XRD patterns are presented in Fig. 1a.

In addition to the change in the XRD peak intensity of the (002) plane, a diffraction peak shift towards the higher angle side is noticed with respect to the number of shock pulses and the emerging values are 26.67, 26.77, 26.81, and 26.83° for the control, 100, 200 and 400 shocks, respectively and the required diffraction shift profile is presented in Fig. 1b. The observed higher angle diffraction peak shift profile against the shock number provides the possible understanding of the enabled enhancement of the local atomic ordering in the rGO samples by
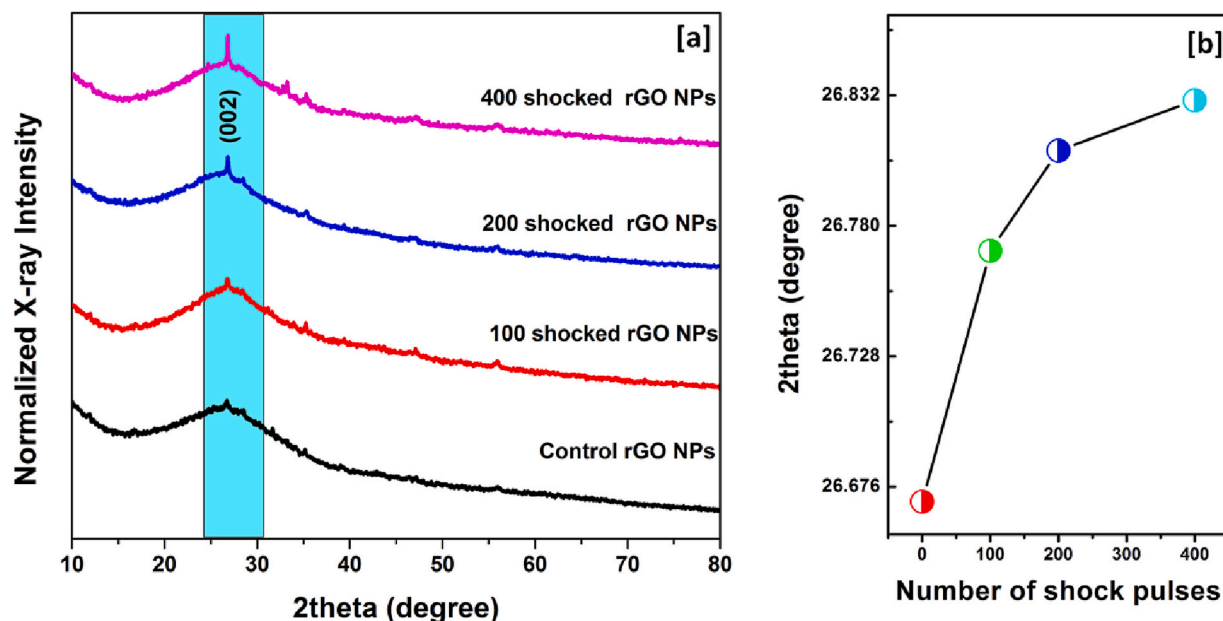
Fig. 1. XRD patterns of the control and shocked rGO NPs (a) XRD patterns (b) diffraction angle shift profile against the number of shock pulses.

the impact of shock waves and note that such kind of atomic ordering process at dynamic shock wave loaded condition is highly unusual. With the intention of obtaining a clear understanding of the atomic ordering in the reduced graphene oxide layers by the impact of shock waves, the Gauss peak fitting process has been performed for the control and the shocked rGO samples such that the peak fitting profiles are shown in Fig. 2(a–d). Based on the obtained fitting parameters, the gown crystalline peak's (002) full-width at half maximum values are considerably reduced against the number of shock pulses and on the other hand, the peak intensity has increased tremendously and the required profiles are shown in Fig. 2f and g. Based on the FWHM and peak intensity profiles against the number of shock pulses, it is authenticated that the atomic ordering of the amorphous rGO NPs has improved considerably under shocked conditions. Note that, in the case of the control rGO sample, the defect density and stacking disorder are very high because of its

amorphous nature whereas the defect density and stacking disorder are reduced at shocked conditions due to the disordered to the ordered phase transitions. As the reasons behind the atomic ordering of rGO samples under shocked conditions are analyzed it is established that, in general, carbon materials may undergo the allotropy phase transitions at very high temperature and pressure such that the phase transitions are highly dependent on the starting phase (Ex; order or disorder phase) and starting form of the carbon materials i.e. graphene, graphite, fullerene and nanotubes etc. [21–27]. In the case of amorphous carbon samples i. e. both graphene and graphite samples, the sp^3 orbital carbon atoms are more than that of the sp^2 orbital carbon atoms which have been very well-studied over the last few decays [21–27].

While the applied supersonic shock waves travel through the test samples, it carries a high temperature enthalpy within it whereby the existing temperature (864 K) and time are sufficient enough to re-
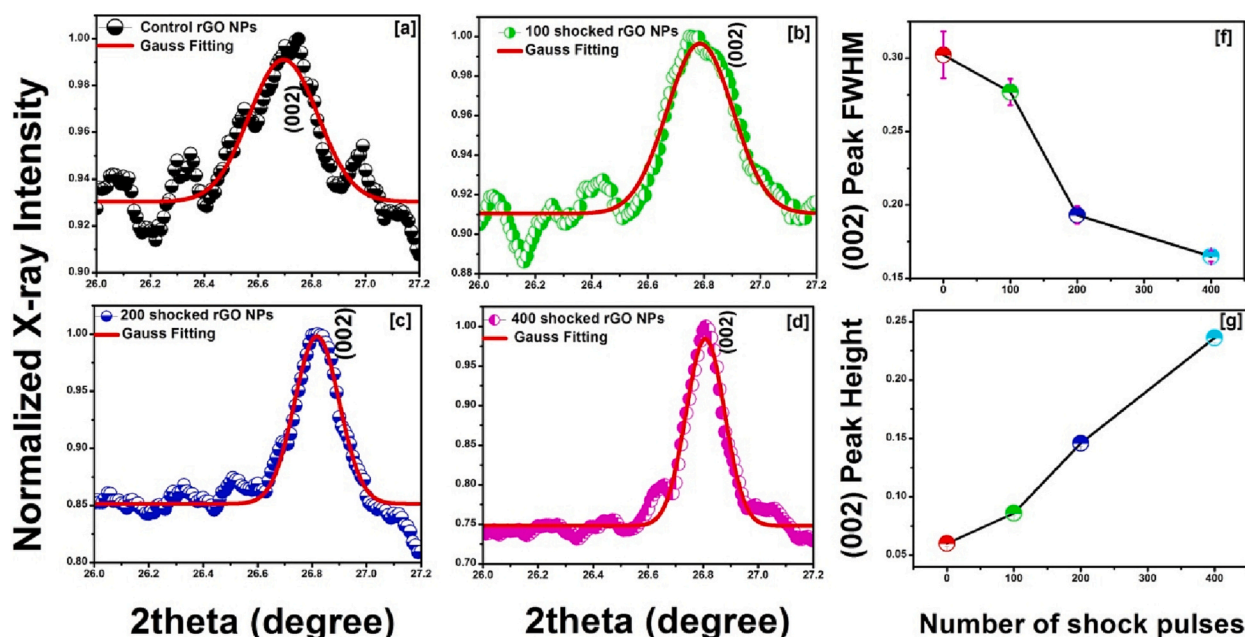

Fig. 2. Gauss peak fitting of the control and shocked samples as well as FWHM and Peak intensity profiles.

crystallize i.e. the prevalent disordered carbon atoms are transformed into the ordered carbon atoms which is based on the shock wave-induced hot-spot nucleation mechanism [39,42]. At this stage, the diffusional reconstructive process can occur because of the shock pressure and temperature thereby the available shear bonds, vacancies, deformation, twin boundaries, and dislocations are significantly reduced such that long-range ordered rGO NPs are produced under shocked conditions. Note that the above-mentioned factors such as shear bonds, vacancies, deformation, twin boundaries, and dislocations are highly dominant according to the observed X-ray peak intensity and due to this reason, diffraction lines are not seen in the control sample. But, when these factors have started to reduce because of the impact of shock waves, the X-ray peak intensity of the (200) plane has started to increase which is clearly reflected by the increment of net crystallinity of the samples. Indeed, the sustained high-pressure and high-temperature conditions promote the artificial nucleation in the disordered samples for which the required temperature is 1000–2000 °C to convert rGO into graphene structures. However, under acoustically shocked circumstances, only a small amount of dynamic temperature is necessary to cause artificial nucleation in the disordered samples [39,42]. Additionally, as the number of shock pulses is increased, the degree of ordering also rises, showing that the shock waves applied give crystals enough time to re-crystallize due to the latent heat produced by the impact of the shock pulses. This disordered to the ordered phase transition has also been seen in multi-wall carbon nanotubes under acoustically shocked conditions [39]. But, the shock wave-induced disordered to the ordered phase conversion is not perfectly attained and a lot of optimization work have to be performed in improving the conversion efficiency.

3.2. Raman spectral results

It is well known that the carbon materials' phase identifications as well as the degree of the order and disorder in the carbon samples can be examined by the Raman spectroscopy whereby the crystal clear picture could be identified on the degree of the order (G-band) and disorder (D-band) as well as their ratio while the ratio is based on the intensity of the G and D bands [21,28]. In addition to that, for a better understanding of the order-disorder phase transitions occurring in the carbon materials, Raman spectroscopic analysis is superior to the basic conventional XRD analysis. So that, the Raman measurements for the control and shocked samples have been performed to realize better the proposed disordered into the ordered phase transitions in the rGO NPs such that the recorded Raman spectra are shown in Fig. 3. The Raman spectra have been observed in the usual backscattering geometry with a micro-Raman spectrometer (Renishaw Ramascope, model 1000) coupled to an optical microscope focusing the λ = 532 nm laser beam to a 2 μm spot diameter. As seen in Fig. 3, the control rGO sample has two characteristics Raman bands that are located at 1381 and 1563 cm^{-1} and they are represented as D and G-band, respectively thereby the observed locations are identified to be well-matched with the previously reported amorphous rGO NPs [40].

The first peak is located at 1381 cm^{-1} (D peak) which is related to the defect and breathing modes of sp^2 rings while the second peak is located at 1563 cm^{-1} (G peak) that originates in the graphite related to doubly degenerate phonon mode (E2g symmetry). Considering the intensity profiles of the D and G bands, the D band has higher normalized intensity than that of the G band which clearly indicates the formation of an amorphous state in rGO samples and these Raman spectral results are corroborated with the XRD results. In Fig. 4, the D and G band peak shift and ID/IG band intensity profile against the impact of shock waves are presented such that, based on the obtained Raman shift profiles, the D band is shifted towards lower energy (Fig. 4a) thereby the values are known to be 1381, 1378, 1365, and 1361 cm^{-1} for the 0,100,200 and 400 shocked rGO samples, respectively. In the case of G-band (Fig. 4b), the Raman shifts are identified to be 1563, 1560, 1547, and 1545 cm^{-1}
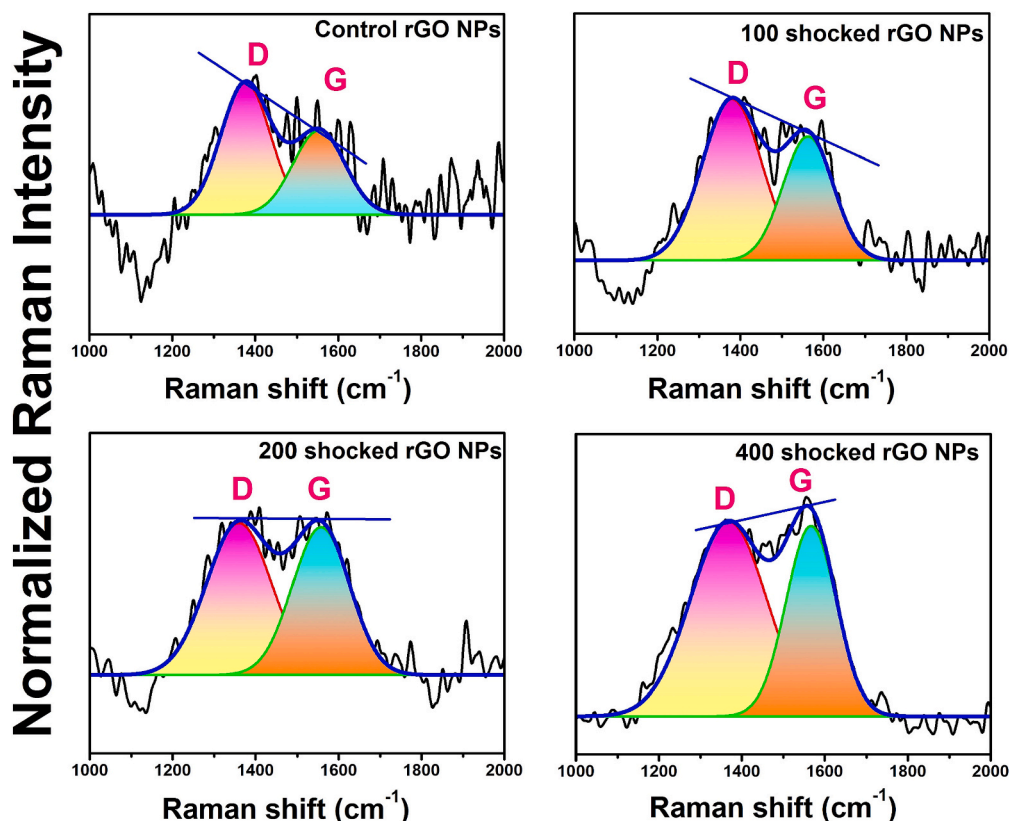

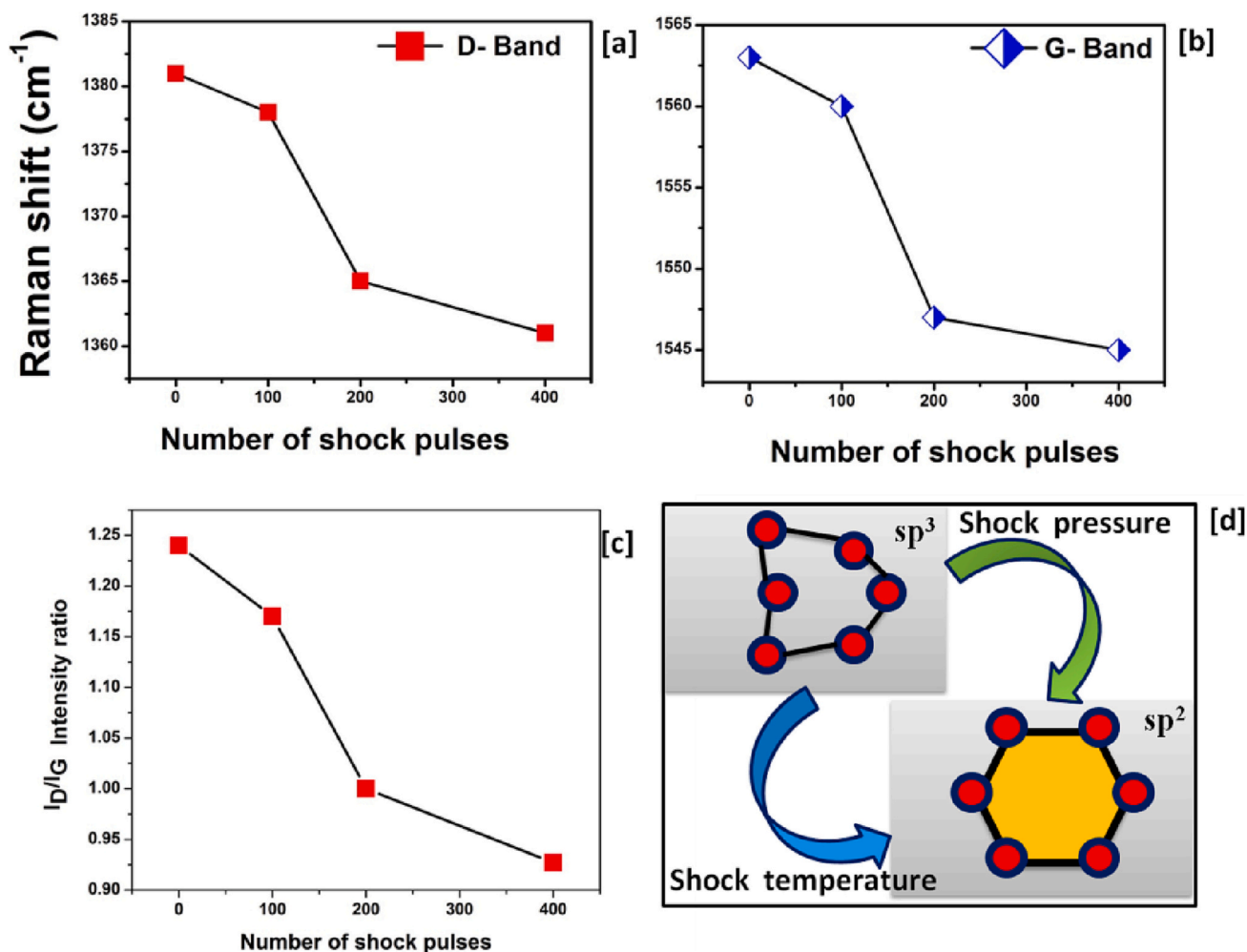**Fig. 3.** D and G bands of the control and shocked rGO NPs.

Fig. 4. (a) D-band shift, (b) G-band shift, (c) ID/IG band ratio for the control and shocked condition (d) schematic representation for the sp^3 to sp^2 conversion.

for the 0, 100, 200 and 400 shocked rGO samples, respectively. More importantly, the ID/IG band intensity ratio profile plays a vital role to justify the degree of order and disorder in the samples such that the required intensity ratio profile against the number of shock pulses is presented in Fig. 4c. Based on the obtained profile, it is evident that the ID/IG band intensity decreases as the number of shock pulses increases, indicating an increase in local order and a better crystalline character than the control rGO samples' amorphous state. Note that the characteristic G band intensity provides the population of sp^2 carbon forms which arise from the C—C bond stretching. According to Fig. 3 and Fig. 4, it is obvious that, under dynamic shocked conditions, the population of sp^3 carbon forms is higher in the amorphous sample whereas the population of sp^3 carbon forms is linearly reduced with respect to the number of shock pulses thereby the net population of the sp^2 carbon forms is increased which paves the way for the disordered to the ordered phase transitions under shocked conditions. The graphical representation of the transformation of sp^3 carbon atoms into sp^2 is shown in Fig. 4d.

The lower wavenumber shift of the G-band clearly indicates that the reduction of amorphous clusters existed in the control samples is due to the dynamic re-crystallization occurring under shocked conditions which influence to convert from the actual graphene layered structures. The possible mechanism for the disordered to the ordered phase transitions is that, when high-pressure and temperature shock pulse is loaded on the samples; it modifies the potential energy on the surface of the rGO samples [43]. At this stage, most of the sp^3 carbons are turned into the sp^2 carbons such that the local atomic sitting positions are altered in the six atom carbon rings which lead to the ordered structures in a time scale of microseconds. In addition to the continuous reduction of the D-band intensity against the shock pulses, the assumptions for the formation of graphene layered structures from the amorphous rGO samples are well-authenticated. Note that, in the case of the reduction process in the graphene oxide NPs, usually; the ID band is reduced thereby IG band intensity is increased based on the removal of the oxygen containing functional groups which normally happens when the test samples are subjected to the thermal heat treatment and as a result, the crystallite size and sp^2 domain concentrations are increased [26,28,43]. Here also, a similar kind of decrement and increment of D and G band intensity is witnessed which clearly indicates the occurrence of the reduction process whereby the increment of grain size and sp^2 carbon concentration is ensured under shocked conditions and it makes the samples as highly reduced GO components such that this kind of behavior is very much required to achieve the pure graphene structures from the graphene oxide structures by the influence of shock waves. In the Raman spectra, the amorphous carbon Raman band usually appears between 500 and 1000 cm^{-1} such that it gives clear details about the amorphous carbon in quantitative aspects [38,44]. Hence, the amorphous carbon Raman band features are provided for the control and shocked rGO samples in Fig. 5 along with its peak area and Raman shift positions with respect to the number of shock pulses. As seen in Fig. 5a, the broad amorphous carbon peak is located at 788 cm^{-1} and after shocked conditions, it got shifted towards the higher wavenumber and the observed Raman band positions are identified to be at 798, 797, 805 cm^{-1} for the respective 100, 200 and 400 shocked conditions. The area
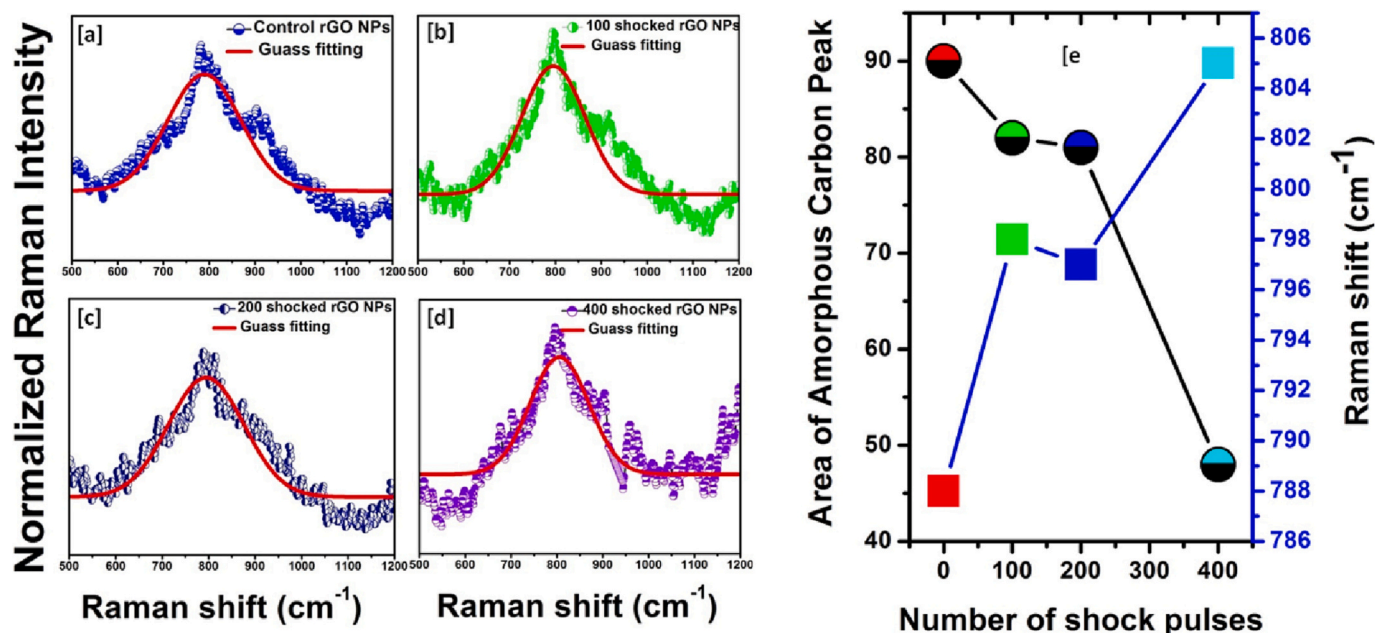
Fig. 5. (a–d) Amorphous carbon peaks fittings of the amorphous carbon bands for the control and shocked samples (d) peak area and Raman peak shift with respect to the number of shock pulses.

under the amorphous peak carbon for the control and shocked samples is calculated using the Gaussian peak fitting method, and based on the peak fitting, the results are 90, 82, 81, and 48, respectively, for the 0, 100, 200, and 400 shocked conditions.

As per the previous discussion regarding the G and D band features, the amorphous carbon is made up of sp^3 hybridization thereby a large area under the amorphous carbon band could be witnessed which represents that the control sample has high sp^3 hybridization carbons. On the other hand, under shocked conditions, the area under the amorphous

carbon band is linearly reduced against the number of shock pulses which amply illustrates the reduction of sp^3 carbon atoms under shocked conditions. Based on the obtained numerical values of the area under the curve for the control and 400 shocked samples, it appears almost 2:1 ratio such that at 400 shocked conditions, 50 % of the sp^3 carbon atoms might have been converted to the sp^2 carbons based on the hot-spot nucleation mechanism.
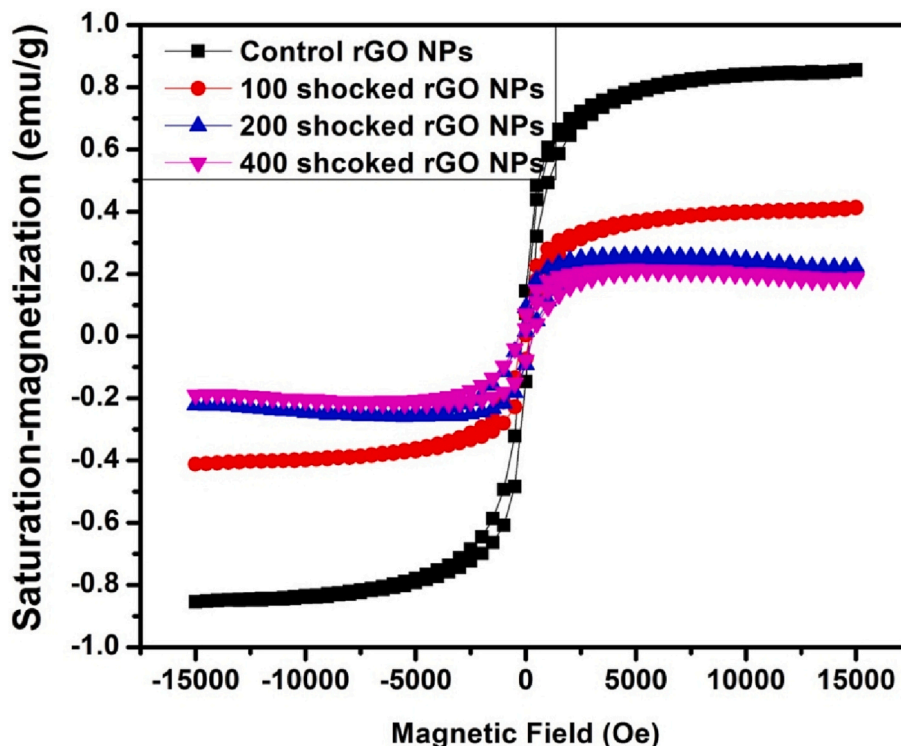

Fig. 6. VSM plots for the control and shocked rGO samples.

3.3. Magnetic properties

Exploring the magnetic properties provides an alternative way to understand the defect density in the carbon materials which include graphite and graphene materials. Hence, the magnetic properties of the control and shocked rGO samples are examined to know more about the disordered to the ordered phase transitions under shocked conditions whereby the observed room temperature magnetic hysteresis loops are presented in Fig. 6.

Several researchers have performed the analysis of magnetic properties for rGO and GO NPs and found several interesting results because of the presence of wide spectra of oxygen components [41,45]. In addition to that, pure graphite and graphene materials are found to have magnetic resonances due to the existence of a variety of atomic level defects within them which are mostly topological defects such as pentagons, heptagons, or their combinations as well as point defects like vacancies and extended defects like edges, cracks, voids etc. [41,45]. Analyzing the obtained M-H loop of the control rGO sample, a weak ferromagnetic behavior is noticed and this kind of weak ferromagnetic behavior occurs mainly because of the sp^3 disordered carbons and the oxygen related components. Better to be aware that even in the rGO samples, a small amount of the oxygen related components may still remain within it and such kind of the oxygen related components may contribute to the total magnetic response [41,45]. In recent years, there has been a lot of research documented regarding the defect-induced weak ferromagnetic state existing in non-magnetic oxide materials [46,47]. Interestingly, under shocked conditions, the possible changes in the M-H loops could be witnessed with respect to the number of shock pulses such that the saturation magnetization is found to have continuously reduced with respect to the number of shock pulses whereby the values are known to be 0.8633, 0.414, 0.2196, and 0.178 emu/g for the 0, 100, 200 and 400 shocks, respectively. Moreover, the value of coercivity increases with respect to the number of shock pulses whereas it remains the same for the 200 and 400 shocked conditions and the relevant plots are portrayed in Fig. 7(a, b). The reduction of the saturation magnetization in rGO samples is mainly attributed to the indication of the formation of the ordered rGO samples under shocked conditions. Because of the increased sp^2 C—C network in the samples, the magnetic moments are highly restricted in the rGO samples thereby the saturation magnetization is linearly reduced with respect to the number of shock pulses such that the obtained results of XRD and Raman are highly consistent with the VSM results.

For more clarity, the relation between the density of sp^2 carbon atoms and saturation magnetization for the control and shocked samples are presented in Fig. 8 wherein it is authenticated that both the parameters are reduced with respect to the number of shock pulses. Hence, it is evident that the increment of the sp^2 carbon atoms reduces the
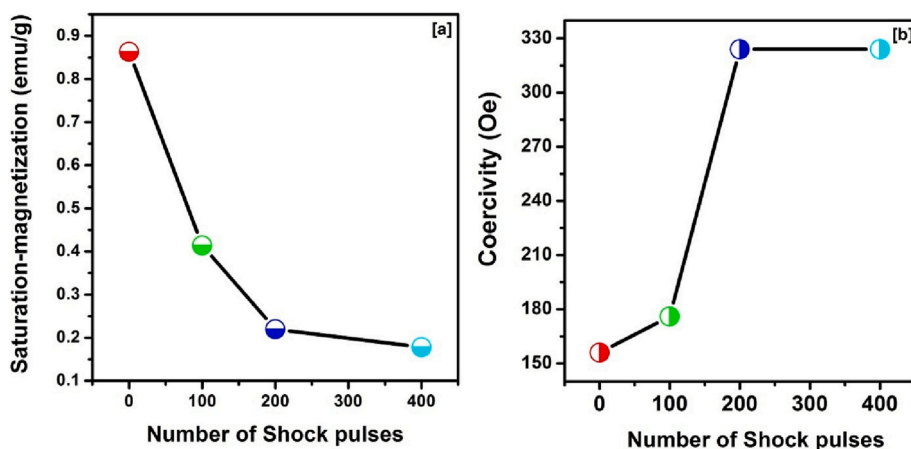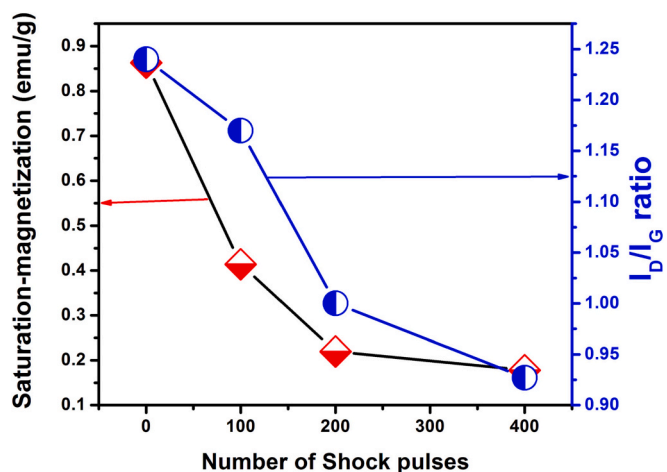
Fig. 8. Relation between the density of sp^2 carbon atoms and saturation magnetization for the control and shocked rGO samples.

saturation magnetization in the rGO sample thereby while disordered to the ordered phase transition occurs, the saturation magnetization is reduced.

3.4. Transmission electron microscopic (TEM) analysis

For a further understanding of the formation of crystalline rGO NPs under shocked conditions, the TEM analysis has been performed for the control and 400-shocked samples such that the obtained TEM images are presented in Fig. 9. As seen in Fig. 9b and c, the absence of FFT pattern and SAED pattern clearly represents that the control sample has amorphous nature, while looking at Fig. 9(d, e and f), significant changes are observed in the surface morphology and atomic structure of rGO NPs at the 400-shocked condition. Note that the occurrence of the highly visible FFT pattern (Fig. 9e) and SAED pattern (Fig. 9f) along the plane (002) clearly shows the formation of the crystalline rGO NPs at the 400 shocked condition and the obtained TEM results are identified to be well corroborated with the XRD and Raman results.

4. Conclusion

In consolidating the prominent features of the current work on carbon-based materials, we have successfully achieved a considerable level of the disordered to the ordered phase transition in graphene layers that have been directly synthesized in the form of rGO NPs under shocked conditions. The XRD pattern line of (002) provides the
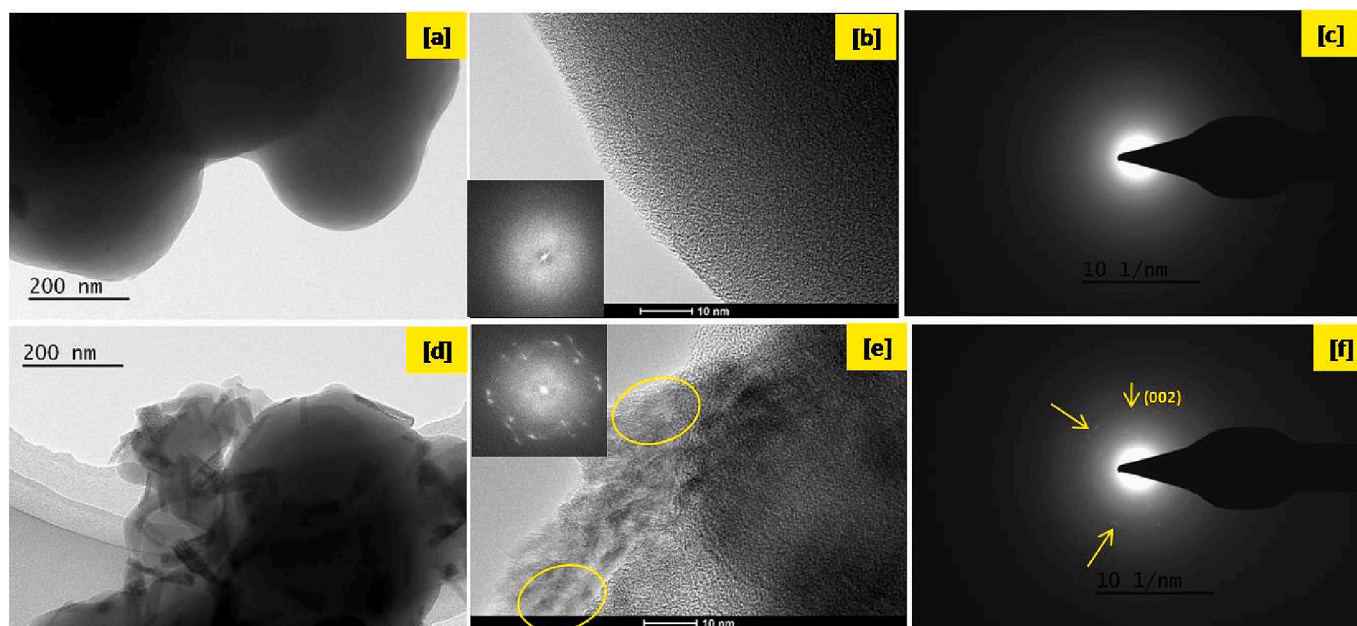
Fig. 7. (a) Saturation magnetization. (b) Coercivity values for 0, 100, 200 and 400 shocked rGO NPs.

Fig. 9. TEM images of the control and shocked rGO samples (a, b, c) the control rGO NPs, (d, e, f) the 400 shocked rGO NPs.

preliminary understanding of the enhancement of the local atomic ordering driven by shock waves thereby removing the amorphous clusters in rGO samples. Raman spectral results demonstrate a clear picture of the above-mentioned local atomic ordering in the rGO samples wherein the D and G band features well agree with the XRD results. Also, the I_D/I_G ratio is linearly reduced with respect to the number of shock pulses such that the values are estimated to be 1.24, 1.17, 1 and 0.927 for 0, 100, 200 and 400 shocks, respectively. Therefore, these values clearly represent the linear increment of sp^2 carbon population and the reduction of the sp^3 carbon population in the samples. The significant reduction of the ID/IG band provides the non-debatable evidence for the atomic ordering in the rGO samples under dynamic shocked conditions. VSM results show the linear reduction of the saturation magnetization against the number of shock pulses which is mainly attributed to the linear increment of sp^2 carbon population with respect to the number of shock pulses. TEM images provide the indispensable authentic proof for the formation of crystalline rGO NPs at 400-shocked condition. To synthesize a pure graphene layer structure, a lot of parameters are needed to be optimized and they are shock pressure, the synthesis process of the rGO NPs, particles' nature and particles' size so that the above-mentioned optimization process is under progress.

Ethics approval

Not applicable.

Consent to participate

All the authors agree to participate.

Informed consent

All people involved in or responsible for the research are informed and consent.

CRediT authorship contribution statement

A. Sivakumar and Lidong Dai - conceptualized the project and Roles/ Writing - original draft. S. Sahaya Jude Dhas - Visualization, Roles/ Writing - original draft. S. A. Martin Britto Dhas- Investigation, Writing-

review & editing. V.Mowlika- sample preparations and characterizations. Raju Suresh Kumar and Abdulrahman I. Almansour helped the data processing and analysis. All the authors discussed the results and commented on the manuscript.

Declaration of competing interest

The authors declare no conflict financial interests.

Data availability

Data will be made available on request.

References

[1] Su Zhi, William L. Shaw, Yu-Run Miao, Sizhu You, Dana D. Dlott, Kenneth S. Suslick, Shock wave chemistry in a metal–organic framework, J. Am. Chem. Soc. 139 (2017) 4619–4622.

[2] Xuan Zhou, Yu-Run Miao, William L. Shaw, Kenneth S. Suslick, Dana D. Dlott, Shock wave energy absorption in metal–organic framework, J. Am. Chem. Soc. 141 (2019) 2220–2223.

[3] A. Sivakumar, S. Reena Devi, S. Sahaya Jude Dhas, R. Mohan Kumar, K. Kamala Bharathi, S.A. Martin Britto Dhas, Switchable phase transformation (orthorhombic–hexagonal) of potassium sulfate single crystal at ambient temperature by shock waves, Cryst. Growth Des. 20 (2020) 7111–7119.

[4] S. Kalaiarasi, A. Sivakumar, S.A. Martin Britto Dhas, M. Jose, Shock wave induced anatase to rutile TiO_2 phase transition using pressure driven shock tube, Mater. Lett. 219 (2018) 72–75.

[5] A. Sivakumar, A. Rita, S. Sahaya Jude Dhas, K.P.J. Reddy, Raju Suresh Kumar, Abdulrahman I. Almansour, Shubhadip Chakraborty, K. Moovendaran, Jayavel Sridhar, S.A. Martin Britto Dhas, Dynamic shock wave driven simultaneous crystallographic and molecular switching between α-Fe_2O_3 and Fe_3O_4 nanoparticles—a new finding, Dalton Trans. 51 (2022) 9159–9166.

[6] Yun-Zhi Tang, Yi Liu, Ji-Xing Gao, Chang-Feng Wang, Bin Wang, Yu-Hui Tan, He-Rui Wen, Reversible structural phase transition, ferroelectric and switchable dielectric properties of an adduct molecule of hexamethylenetetramine ferrocene carboxylic acid, RSC Adv. 7 (2017) 41369.

[7] M.A. Ahlam, M.N. Ravishankar, N. Vijaya, G. Govindaraj, Siddaramaiah, A.P. Gnana Prakash, Investigation of gamma radiation effect on chemical properties and

surface morphology of some nonlinear optical (NLO) single crystals, Nuc. Inst. Meth. Phys. Res B 278 (2012) 26–33.

[8] Xiao Dong, Ning Li, Zhen Zhu, Hezhu Shao, Ximing Rong, Cong Liang, Haibin Sun, Guojin Feng, Li Zhao, Jun Zhuang, A nitrogen-hyperdoped silicon material formed by femtosecond laser irradiation, Appl. Phys. Lett. 104 (2014), 091907.

[9] Quanjun Li, Bingbing Liu, Lin Wang, Dongmei Li, Ran Liu, Bo Zou, Tian Cui, Guangtian Zou, Yue Meng, Ho-kwang Mao, et al., Pressure-induced morphization and polyamorphism in one-dimensional single-crystal TiO_2 nanomaterials, J. Phys. Chem. Lett. 1 (2010) 309–314.

[10] Yun-Zhi Tang, Yin-Mei Yu, Jian-Bo Xiong, Yu-Hui Tan, He-Rui Wen, Unusual high temperature reversible phase transition behavior, structures and dielectric-ferroelectric properties of two new crown ether clathrates, J. Am. Chem. Soc. 137 (41) (2015) 13345–13351.

[11] Xiaoli Huang, Defang Duan, Kai Wang, Xinyi Yang, Shuqing Jiang, Wenbo Li, Fangfei Li, Qiang Zhou, Xilian Jin, Bo Zou, Bingbing Liu, Tian Cui, Structural and electronic changes of $SnBr_4$ under high pressure, J. Phys. Chem. C 117 (2013) 8381–8387.

[12] A.V. Krasheninnikov, K. Nordlund, Ion and electron irradiation-induced effects in nanostructured materials, J. Appl. Phys. 107 (2010), 071301.

[13] Sudip K. Deb, Martin Wilding, Maddury Somayazulu, Paul F. McMillan, Pressure-induced amorphization and anamorphous to amorphous transition in densified porous silicon, Nature. 414 (2001) 528–530.

[14] Lijun Zhang, Yanchao Wang, Jian Lv, Yanming Ma, Materials discovery at high pressures, Nat. Rev. Mater. 2 (2017) 17005.

[15] O.O. Kurakevych, Y. Le Godec, T.A. Strobel, D.Y. Kim, W.A. Crichton, J. Guignard, Exploring silicon allotropy by high pressure–high temperature conditions, J. Phys. Conf. Ser. 950 (2017), 022006.

[16] M.J. Crane, A. Petrone, R.A. Beck, M.B. Lim, X. Zhou, X. Li, R.M. Stroud, P. J. Pauzauskie, High-pressure, high-temperature molecular doping of nanodiamond, Sci. Adv. 5 (2019) 6073.

[17] M. Corrias, Ph. Serp, Ph. Kalck, G. Dechambre, J.L. Lacout, C. Castiglioni, Y. Kihn, High purity multiwalled carbon nanotubes under high pressure and high temperature, Carbon 41 (2003) 2361–2367.

[18] Andrea C. Ferrari, Raman spectroscopy of graphene and graphite: disorder, electron–phonon coupling, doping and nonadiabatic effects, Solid State Commun. 143 (2007) 47–57.

[19] Shaowen Chen, Minhao He, Ya-Hui Zhang, Valerie Hsieh, Zaiyao Fei, Electrically tunable correlated and topological states in twisted monolayer–bilayer graphene, Nat. Phys. 17 (2021) 374–380.

[20] Jçrg J. Schneider, Transforming amorphous into crystalline carbon: observing how graphene grows, ChemCatChem 3 (2011) 1119–1120.

[21] Mingguang Yao, Zhigang Wang, Bingbing Liu, et al., Raman signature to identify the structural transition of single-wall carbon nanotubes under high pressure, Phys. Rev. B 78 (2008), 205411.

[22] Chen Liang-Chen, Wang Li-Jun, Tang Dong-Sheng, Xie Si-Shen, Jin Chang-Qing, X-ray diffraction study of carbon nanotubes under high pressure, Chin. Phys. Lett. 18 (2001) 577.

[23] Teawon Kim, Jaegeun Lee, Kun-Hong Lee, Full graphitization of amorphous carbon by microwave heating, RSC Adv. 6 (2016) 24667.

[24] Koji Asaka, Motoyuki Karita, Yahachi Saito, Graphitization of amorphous carbon on a multiwall carbon nanotube surface by catalyst-free heating, Appl. Phys. Lett. 99 (2011), 091907.

[25] P.D. Kichambare, L.C. Chen, C.T. Wang, K.J. Ma, C.T. Wu, K.H. Chen, Laser irradiation of carbon nanotubes, Mater. Phys. Chem 72 (2001) 218–222.

[26] B. Arman, Q. An, S.N. Luo, T.G. Desai, D.L. Tonks, T. Çağın, W.A. Goddard, Dynamic response of phenolic resin and its carbon-nanotube composites to shock wave loading, J. Appl. Phys. 109 (2011), 013503.

[27] V.V. Milyavskiy, A.V. Utkin, A.Z. Zhuk, V.V. Yakushev, V.E. Fortov, Shock compressibility and shock-induced phase transitions of C_{60} fullerite, Diam. Relat. Mater. 14 (2005) 1920–1923.

[28] David Veysset, Thomas Pezeril, Steve Kooi, Alain Bulou, Keith Nelson, Shock-wave induced formation of nano-crystalline graphite from highly ordered pyrolytic graphite, Appl. Phys. Lett. 106 (2015), 161902.

[29] Shin-Ichi Hirano, Kazuaki Shimono, Shigeharu Naka, Diamond formation from glassy carbon under high pressure and temperature conditions, J. Mater. Sci. 17 (1982) 1856–1862.

[30] Xu Chao, Duanwei He, Haikuo Wang, Junwei Guan, Chunmei Liu, Fang Peng, Wendan Wang, Zili Kou, Kai He, Xiaozhi Yan, Yan Bi, Lei Liu, Fengjiao Li, Bo Hui, Nano-polycrystalline diamond formation under ultra-high pressure, Int. J. Refract. Hard. Met 36 (2013) 232–237.

[31] A. Sivakumar, S. Soundarya, S. Sahaya Jude Dhas, K. Kamala Bharathi, S.A. Martin Britto Dhas, Shock wave driven solid state phase transformation of Co_3O_4 to CoO nanoparticles, J. Phys. Chem. C 124 (2020) 10755–10763.

[32] A. Sivakumar, P. Shailaja, S. Sahaya Jude Dhas, P. Sivaprakash, Abdulrahman I. Almansour, Raju Suresh Kumar, N. Arumugam, Arumugam, S. Chakraborty, S.A. Martin Britto Dhas, Dynamic shock wave-induced switchable phase transition of magnesium sulfate heptahydrate, Cryst. Growth Des. 21 (2021) 5050–5057.

[33] V. Mowlika, C.S. Naveen, A.R. Phani, A. Sivakumar, S.A. Martin Britto Dhas, R. Robert, Shock wave induced magnetic phase transition in cobalt ferrite nanoparticles, Mater. Chem. Phys. 275 (2022), 125300.

[34] A. Sivakumar, P. Shailaja, M. Nandhini, S. Sahaya Jude Dhas, Raju Suresh Kumar, Abdulrahman I. Almansour, Natarajan Arumugam, Shubhadip Chakraborty, S.A. Martin Britto Dhas, Ternary switchable phase transition of $CaCO_3$ by shock waves, Ceram. Int. 48 (2022) 8457–8465.

[35] A. Sivakumar, S. Sahaya Jude Dhas, P. Sivaprakash, S. Prabhu, K. Moovendaran, A. Murugeswari, S. Arumugam, S.A. Martin Britto Dhas, Shock wave induced conformational phase transition of L-leucine, J. Mol. Struct 1271 (2022), 134033.

[36] N. Koteeswara Reddy, V. Jayaram, E. Arunan, Y.B. Kwon, W.J. Moon, K.P.J. Reddy, Investigations on high enthalpy shock wave exposed graphitic carbon nanoparticles, Diam. Relat. Mater. 35 (2013) 53–57.

[37] L. Biennier, V. Jayaram, N. Suas-David, R. Georges, M. Kiran Singh, E. Arunan, S. Kassi, E. Dartois, K.P.J. Reddy, Shock-wave processing of C_{60} in hydrogen, A&A 599 (2017) A42.

[38] Arijit Roy, Surendra Vikram Singh, M. Ambresh, D. Sahu, J.K. Meka, R. Ramachandran, P. Samarth, S. Pavithraa, V. Jayaram, H. Hill, J. Cami, B. N. Rajasekhar, P. Janardhan, N.J. Anil Bhardwaj, B. Sivaraman Mason, Shock processing of amorphous carbon nanodust, Adv. Space Res. 70 (2022) 2571–2581.

[39] A. Sivakumar, S. Sahaya Jude Dhas, T. Pazhanivel, Abdulrahman I. Almansour, Raju Suresh Kumar, Natarajan Arumugam, C. Justin Raj, S.A. Martin Britto Dhas, Phase transformation of amorphous to crystalline of multiwall carbon nanotubes by shock waves, Cryst. Growth Des. 21 (2021) 1617–1624.

[40] S.K. Sarkar, K.K. Raul, S.S. Pradhan, S. Basu, A. Nayak, Magnetic properties of graphite oxide and reduced graphene oxide, Phys. E. 64 (2014) 78–82.

[41] Ana Elisa Ferreira Oliveira, Guilherme Bettio Braga, Cesar Ricardo Teixeira Tarley, Arnaldo Cesar Pereira, Thermally reduced graphene oxide: synthesis, studies and characterization, J. Mater. Sci. 53 (2018) 12005–12015.

[42] D.G. Morris, An investigation of the shock induced transformation of graphite to diamond, J. Appl. Phys. 51 (1980) 2059.

[43] J. Gaudin, O. Peyrusse, J. Chalupsky, M. Toufarova, L. Vysin, V. Hajkov, R. Sobierajski, T. Burian, et al., Amorphous to crystalline phase transition in carbon induced by intense femtosecond X-ray free-electron laser pulses, Phys. Rev. B 86 (2012), 024103.

[44] Teodor Milenov, Ivalina Avramova, Deposition of graphene by sublimation of pyrolytic carbon, Opt. Quant. Electron. 47 (2015) 851–863.

[45] David O. Idisi, James A. Oke, Evan M. Benecha, Sabato J. Moloi, Sekhar C. Ray, Magnetic properties of graphene oxide functionalized with "Au" and "Fe_2O_3" nanoparticles: a comparative study, Mater. Today. Proc. 44 (2021) 5037–5043.

[46] Michael Coey, Karl Ackland, Munuswamy Venkatesan, Siddhartha Sen, Collective magnetic response of CeO_2 nanoparticles, Nat. Phys. 12 (2016) 694–699.

[47] Karl Ackland, J.M.D. Coey, Room temperature magnetism in CeO_2—a review, Phys. Rep. 746 (2018) 1–39.